Functional reflective polarizer for augmented reality and color vision deficiency

Ruidong Zhu, Guanjun Tan, Jiamin Yuan, and Shin-Tson Wu*

College of Optics and Photonics, University of Central Florida, Orlando, Florida 32816, USA
*swu@ucf.edu

Abstract: We report a functional reflective polarizer that can be incorporated into a compact augmented reality system. The design principle of the functional reflective polarizer is explained and two design examples are illustrated. In the first example, with the specially designed functional reflective polarizer, the transmittance of the augment reality system is relatively high as compared to a polarizing beam splitter or a conventional reflective polarizer. Such a functional reflective polarizer can also be used for vehicular displays. For the second example, the functional reflective polarizer is specially tailored to help those people with color vision deficiency.

OCIS codes: (310.0310) Thin films; (120.4820) Optical systems; (330.1720) Color vision.

References and links

1. J. P. Rolland and H. Fuchs, "Optical versus video see-through head-mounted displays in medical visualization," Presence-Teleop. Virt. **9**(3), 287–309 (2000).
2. A. Olwal, C. Lindfors, J. Gustafsson, T. Kjellberg, and L. Mattsson, "ASTOR: An autostereoscopic optical see-through augmented reality system," in *Proceedings of the 4th IEEE/ACM International Symposium on Mixed and Augmented Reality* (IEEE Computer Society, 2005), pp. 24–27.
3. T. Sielhorst, M. Feuerstein, and N. Navab, "Advanced medical displays: A literature review of augmented reality," J. Disp. Technol. **4**(4), 451–467 (2008).
4. F. Zhou, H. B.-L. Duh, and M. Billinghurst, "Trends in augmented reality tracking, interaction and display: A review of ten years of ISMAR," in *Proceedings of the 7th IEEE/ACM International Symposium on Mixed and Augmented Reality* (IEEE Computer Society, 2008), 193–202.
5. X. Hu and H. Hua, "High-resolution optical see-through multi-focal-plane head-mounted display using freeform optics," Opt. Express **22**(11), 13896–13903 (2014).
6. S. Lee, X. Hu, and H. Hua, "Effects of optical combiner and IPD change for convergence on near-field depth perception in an optical see-through HMD," IEEE Trans. Vis. Comput. Graph. **99**, 1 (2015).
7. R. Zhang and H. Hua, "Characterizing polarization management in a p-HMPD system," Appl. Opt. **47**(4), 512–522 (2008).
8. Y. Li, T. X. Wu, and S.-T. Wu, "Design optimization of reflective polarizers for LCD backlight recycling," J. Disp. Technol. **5**(8), 335–340 (2009).
9. M. F. Weber, C. A. Stover, L. R. Gilbert, T. J. Nevitt, and A. J. Ouderkirk, "Giant birefringent optics in multilayer polymer mirrors," Science **287**(5462), 2451–2456 (2000).
10. M. Alpern and T. Wake, "Cone pigments in human deutan colour vision defects," J. Physiol. **266**(3), 595–612 (1977).
11. S. L. Merbs and J. Nathans, "Absorption spectra of human cone pigments," Nature **356**(6368), 433–435 (1992).
12. M. Neitz and J. Neitz, "Molecular genetics of color vision and color vision defects," Arch. Ophthalmol. **118**(5), 691–700 (2000).
13. T. Alfrey, E. F. Gurnee, and W. J. Schrenk, "Physical optics of iridescent multilayered plastic films," Polym. Eng. Sci. **9**(6), 400–404 (1969).
14. J. Zhang, T. P. Lodge, and C. W. Macosko, "Interfacial slip reduces polymer-polymer adhesion during coextrusion," J. Rheol. (N.Y.N.Y.) **50**(1), 41–57 (2006).
15. J. Dooley, "Determining the processability of multilayer coextruded structures," in *PLACE Conference*, (TAPPI, 2007), 16–20.
16. D. W. Berreman, "Optics in stratified and anisotropic media: 4×4-matrix formulation," J. Opt. Soc. Am. **62**(4), 502–510 (1972).
17. Y. Huang, T. X. Wu, and S.-T. Wu, "Simulations of liquid-crystal Fabry–Perot etalons by an improved 4×4 matrix method," J. Appl. Phys. **93**(5), 2490–2495 (2003).
18. P. Yeh, *Optical Waves in Layered Media* (Wiley, 1988).

#258893 Received 3 Feb 2016; accepted 29 Feb 2016; published 3 Mar 2016

19. J. Li, G. Baird, Y.-H. Lin, H. Ren, and S.-T. Wu, "Refractive-index matching between liquid crystals and photopolymers," J. Soc. Inf. Disp. **13**(12), 1017–1026 (2005).
20. J. Li and S.-T. Wu, "Extended cauchy equations for the refractive indices of liquid crystals," J. Appl. Phys. **95**(3), 896–901 (2004).
21. E. K. Macdonald and M. P. Shaver, "Intrinsic high refractive index polymers," Polym. Int. **64**(1), 6–14 (2015).
22. T. Higashihara and M. Ueda, "Recent progress in high refractive index polymers," Macromolecules **48**(7), 1915–1929 (2015).
23. K. Masaoka, Y. Nishida, M. Sugawara, and E. Nakasu, "Design of primaries for a wide-gamut television colorimetry," IEEE Trans. Broadcast **56**(4), 452–457 (2010).
24. R. Zhu, Z. Luo, H. Chen, Y. Dong, and S.-T. Wu, "Realizing Rec. 2020 color gamut with quantum dot displays," Opt. Express **23**(18), 23680–23693 (2015).
25. J. I. You and K.-C. Park, "Image processing with color compensation using LCD display for color vision deficiency," J. Disp. Technol. **PP**, 189 (2015).
26. G. M. Machado, M. M. Oliveira, and L. A. F. Fernandes, "A physiologically-based model for simulation of color vision deficiency," IEEE Trans. Vis. Comput. Graph. **15**(6), 1291–1298 (2009).
27. E. Tanuwidjaja, D. Huynh, K. Koa, C. Nguyen, C. Shao, P. Torbett, C. Emmenegger, and N. Weibel, "Chroma: A wearable augmented-reality solution for color blindness," in *Proceedings of the 2014 ACM International Joint Conference on Pervasive and Ubiquitous Computing* (ACM, 2014), pp. 799–810.
28. D. H. Brainard, H. Jiang, N. P. Cottaris, F. Rieke, E. J. Chichilnisky, J. E. Farrell, and B. A. Wandell, "Isetbio: Computational tools for modeling early human vision," in *Imaging and Applied Optics 2015*, OSA Technical Digest (online) (Optical Society of America, 2015), paper IT4A.4.
29. H. Brettel, F. Viénot, and J. D. Mollon, "Computerized simulation of color appearance for dichromats," J. Opt. Soc. Am. A **14**(10), 2647–2655 (1997).
30. R. L. Donofrio, "Review paper: The Helmholtz-K ohlrausch effect," J. Soc. Inf. Disp. **19**(10), 658–664 (2011).
31. J. F. Van Derlofske, J. M. Hillis, A. Lathrop, J. Wheatley, J. Thielen, and G. Benoit, "19.1: Invited paper: Illuminating the value of larger color gamuts for quantum dot displays," SID Symp. Dig. Tech. Pap. **45**(1), 237–240 (2014).

1. Introduction

In an optical see-through augmented reality (AR) system [1–6], polarization management is of vital importance to improve the ambient contrast ratio and brightness of the display [7]. A key component for polarization management is polarizing beam splitter (PBS). Even though the PBS has exceptional performance, it makes the whole system bulky and heavy. Whereas compactness and lightweight are crucial for the head-mounted AR display. Recently with the advanced fabrication technology, it is possible to laminate a thin reflective polarizer onto an optical surface with good uniformity [8, 9]. If we replace the PBS with a reflective polarizer, the AR system will work equally well but with a much thinner profile and lighter weight.

In this paper, we designed two kinds of functional reflective polarizers for different applications. The first design improves the transmittance of an AR system, while the second design helps those people with color vision deficiency (CVD) [10–12]. Our functional reflective polarizers work well as long as the display light is polarized. Besides AR system, our functional reflective polarizer can also be integrated into a vehicle by laminating it to the windshield for improving the ambient contrast ratio of heads-up displays.

2. The AR system

Figure 1 depicts a simplified device configuration of our AR system. Let us first discuss the pros and cons of using a broadband reflective polarizer, instead of our new functional reflective polarizer. The reflective polarizer is laminated on the back surface of the eyeglass or goggle. The unpolarized ambient light partially passes through the eyeglass and reflective polarizer while the polarized display light (e.g. from a liquid crystal display) is reflected by the reflective polarizer. In this sense, the AR system effectively combines the displayed images with the outside world and the reflective polarizer functions similarly to the PBS. However, the reflective polarizer suffers the same problem as PBS: only about half of the unpolarized ambient light is transmitted while the other half is reflected back. The decreased transmittance makes it difficult for inconspicuous display systems where the display has to disappear into the background. Moreover, such a reflective polarizer is unsuitable for vehicular display because of its low transmittance. To remedy the abovementioned problems,

#258893 Received 3 Feb 2016; accepted 29 Feb 2016; published 3 Mar 2016

in the following section we propose to replace the reflective polarizer with a functional reflective polarizer.

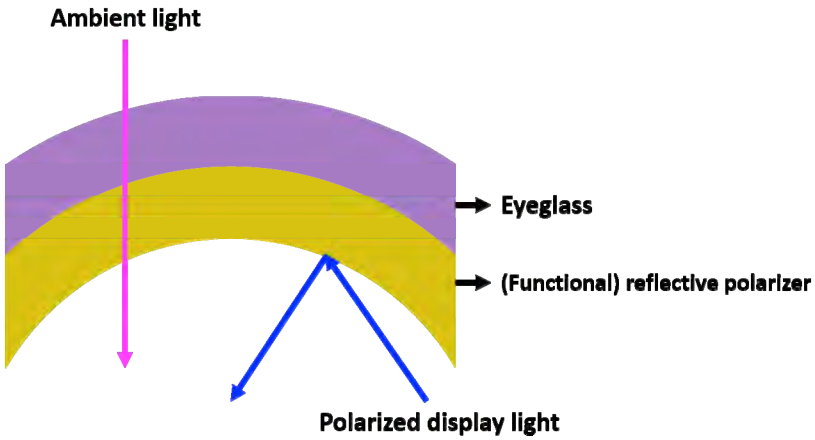

Fig. 1. Structure of the proposed AR system.

3. Design principle of the functional reflective polarizer

Reflective polarizer, also known as dual brightness enhancement film (DBEF) [8, 9], is fabricated by polymer coextrusion [13–15] and has been widely used in liquid crystal display backlight system for enhancing the optical efficiency. It consists of alternating uniaxial/isotropic layers, as shown in Fig. 2(a). The refractive index of the isotropic material is n_1, as for the uniaxial material the ordinary refractive index is n_1 and the extraordinary refractive index is n_2. The uniaxial material is aligned along the *x*-axis. For the light polarized along the *x*-axis, it sees alternating refractive index and the stack works as a highly reflective film. While for the light polarized along the *y*-axis, it sees only n_1 so that the structure works as a high transmittance film. In this way, the reflective polarizer would reflect the *x*-polarized light while transmitting *y*-polarized light. The reflective polarizer can be designed by the 4 × 4 method [16, 17] developed for analyzing uniaxial liquid crystals. However, as there is no refractive index change along the *y* direction, it is not possible to control the transmittance/reflectance of the *y*-polarized light. The most straightforward way to control the transmittance/reflectance of the *y*-polarized light is to introduce refractive index variation in the *y* direction. However, designing such a functional reflective polarizer that controls the *x*-polarized light and *y*-polarized light simultaneously is quite challenging by the 4 × 4 method. To help design the functional reflective polarizer, we need to take a look at the 4 × 4 method, which is used for analyzing liquid crystal display, and the transfer matrix approach [18], which is used in general for thin film coating design. We can tell that the main difference between the transfer matrix approach and the 4 × 4 method is that in the latter we introduce polar and azimuthal angles to describe the tilt and twist deformations of the LC directors. The incurred LC reorientation will introduce polarization rotation effect into the system. However, in the case of functional reflective polarizer, the problem can be greatly simplified if we assume that the uniaxial material is oriented along *x*-axis or *y*-axis. Then the polarization rotation effect would be negligible and the design process of the functional reflective polarizer can be simplified as outlined in the following:

1. Designing two thin film coatings with different transmittance/reflectance properties using isotropic materials m_1 and m_2 with refractive index n_1 and n_2, respectively. If we name the two coatings Stack 1 and Stack 2, it is required that the two thin film coatings having the same thickness.

#258893 Received 3 Feb 2016; accepted 29 Feb 2016; published 3 Mar 2016

2. Convert the two thin film coatings to functional reflective polarizer. Compare the two stacks: at the same thickness, if both stacks have the refractive index of n_1, then for the functional reflective polarizer, at this thickness we should use material m_1. Similarly, if both stacks have the refractive indices of n_2, we should use isotropic material m_2. In addition, if for Stack 1 the refractive index is n_1 and for Stack 2 the refractive index is n_2, then we should use the uniaxial material m_3 ($n_e = n_2$ and $n_o = n_1$) with the long axis aligned along the *y* direction. If on the contrary, the refractive index for Stack 1 is n_2 and for Stack 2 the refractive index is n_1, then the uniaxial material should be aligned along the *x* direction. This conversion procedure is illustrated in Fig. 2(b).

3. Recalculate the transmittance and reflectivity of the functional reflective polarizer with the 4 × 4 method.

4. Fine-tune the stack design of the functional reflective polarizer.

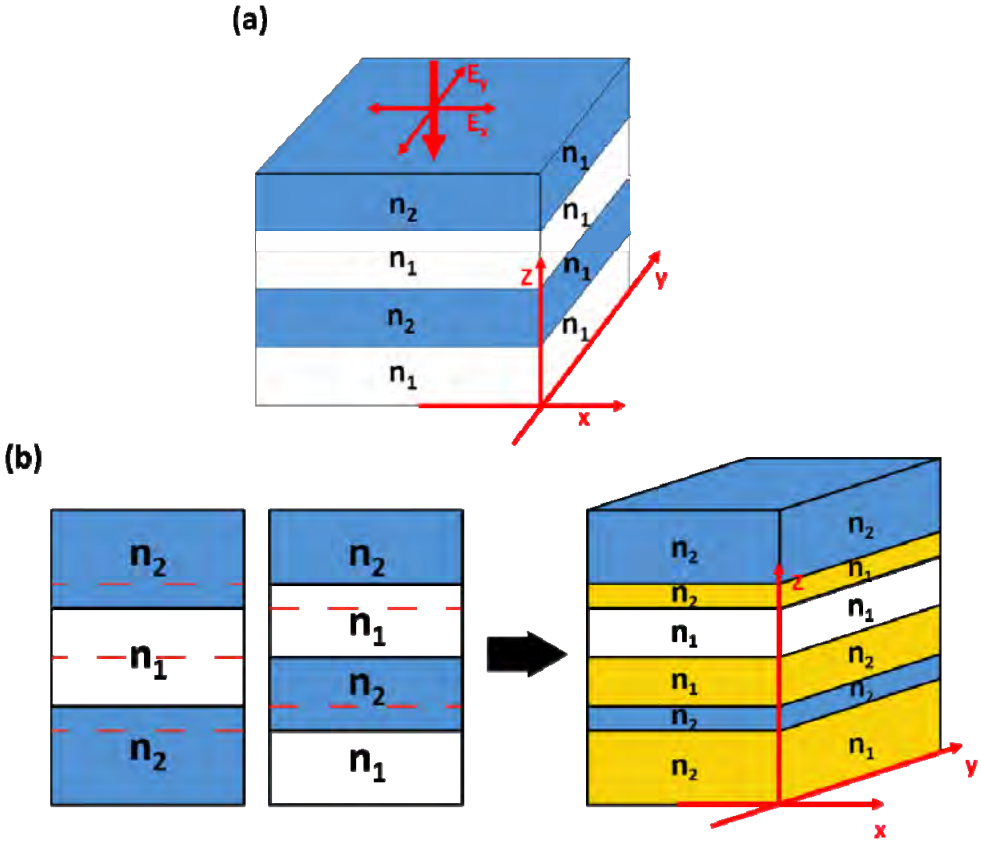

Fig. 2. (a) Structure of the regular reflective polarizer and (b) the principle of converting two thin film coatings to a single functional reflective polarizer: materials m_1, m_2 and m_3 are drawn in white, blue and yellow, respectively.

With the abovementioned approach, it is possible to design the functional reflective polarizer with three materials: a uniaxial material with $n_e = n_2$ and $n_o = n_1$ and two isotropic materials with matched refractive indices of n_1 and n_2, respectively. Throughout this paper, the isotropic materials we used in our design simulation are NOA81 (n = 1.57) [19, 20] and polyferrocenes (n = 1.82) [21, 22], and the uniaxial material is liquid crystal polymeric film

#258893 Received 3 Feb 2016; accepted 29 Feb 2016; published 3 Mar 2016

(BL038, n_e = 1.82, n_o = 1.57) [19, 20]. In real fabrication we can also select other materials as long as the refractive index matching condition is satisfied and the birefringence of the uniaxial material is large enough [8, 9]. The most important advantage of our approach is that there are quite a few optimization approaches for fast thin film coating designs.

4. Functional reflective polarizer for inconspicuous AR system/vehicular display

With the abovementioned approach, we can design different functional reflective polarizers for different applications. The first example is a functional reflective polarizer for inconspicuous AR system and vehicular display. For these applications, the overall transmittance of the ambient light should be high while keeping high reflectivity for the display light. To achieve this goal, we modify the structure based on Fig. 2(a). In the *y* direction, the refractive index is n_1 so that the *y*-polarized light is transmitted. In the x direction, we modify the stack design to make it working as a multiband notched filter. That is to say, the *x*-polarized incident light centered at 467nm, 532nm and 630nm will be reflected back, but the light at other wavelength (both polarizations) will have high transmittance. For such a functional reflective polarizer, we only use two types of materials: BL038-based polymeric film and NOA81. Such a functional reflective polarizer consists of 103 layers with a total thickness of 8.04 μm. As mentioned in Sec. 2, each layer thickness is optimized by the transfer matrix method and validated through the 4 × 4 matrix method. Detail parameters are not listed here due to space limit. Figure 3(a) shows the simulated transmission spectra using the 4 × 4 matrix method. In our design, we assume that the display emits a linearly polarized light along the *x* direction.

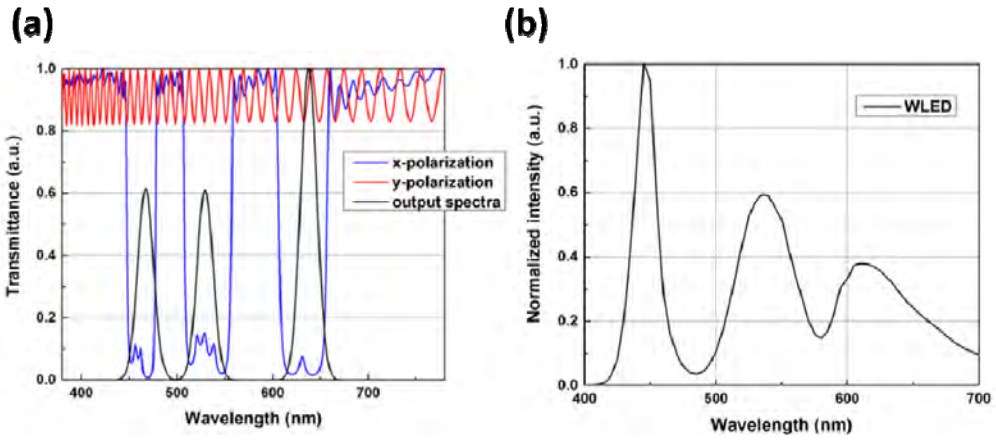

Fig. 3. (a) Simulated transmittance of the functional reflective polarizer and the normalized output spectra of the display panel, and (b) the output spectra of a WLED embedded LCD.

The notched band is so designed that it covers as much the output spectra from the display side as possible. In this sense, the reflectivity of the display will not be compromised. Here the display is a quantum dot (QD)-enhanced LCD where the RGB color primaries are tailored to cover the Rec. 2020 color gamut specified for ultra-high definition (UHD) displays [23, 24]. As Fig. 3(a) depicts, the notched band can effectively cover the output spectra of the display.

The transmittance of the reflective polarizer can be defined as:

$$T_i = \int_{\lambda_1}^{\lambda_2} t_i(\lambda) I_i(\lambda) d\lambda \Big/ \int_{\lambda_1}^{\lambda_2} I_i(\lambda) d\lambda. \quad (1)$$

#258893 Received 3 Feb 2016; accepted 29 Feb 2016; published 3 Mar 2016

In Eq. (1), $i = x,y$ represents the x and y polarization, respectively, $t(\lambda)$ is the wavelength dependent transmittance and $I(\lambda)$ is the spectra of the light. For the unpolarized ambient light, the total transmittance T can be expressed as:

$$T = \frac{1}{2}(T_x + T_y) = \frac{1}{2}\left(\int_{\lambda_1}^{\lambda_2} [t_x(\lambda) + t_y(\lambda)] I(\lambda) d\lambda \Big/ \int_{\lambda_1}^{\lambda_2} I(\lambda) d\lambda \right). \quad (2)$$

Similarly, for the x-polarized display light the reflectivity of the display light R_D can be calculated as:

$$R_D = 1 - T_D = 1 - \int_{\lambda_1}^{\lambda_2} t_x(\lambda) I_D(\lambda) d\lambda \Big/ \int_{\lambda_1}^{\lambda_2} I_D(\lambda) d\lambda. \quad (3)$$

In Eq. (3), T_D is the overall transmittance of the display light and $I_D(\lambda)$ is the spectra of the display light.

If we assume the ambient light is D65 (white light) and the display output spectrum is that shown in Fig. 3(a), with Eqs. (1) and (2) we find the transmittance T_x = 0.6286, T_y = 0.9089 and T = 0.7692. For the *x*-polarized display light, the reflectivity R_D is 0.9069. For a regular ideal reflective polarizer, T_x = 0, T_y = 1, T = 0.5 and R_D = 1. Comparing these results, we can see that the functional reflective polarizer has ~54% transmittance gain in terms of ambient light and the reflectivity loss for the display light is only ~10%. Such exceptional performance makes the functional reflective polarizer ideal for inconspicuous display and vehicular display.

In Fig. 3(a), the sinusoidal-like transmittance curve along the *y*-direction comes from the constructive and destructive interferences between the top and bottom surfaces, and the average transmittance can be estimated if we ignore the interference between the top and bottom surfaces. When light encounters the top surface, the reflectivity can be calculated by the Snell's law [18] as

$$R = \frac{(n-1)^2}{(n+1)^2}, \quad (4)$$

here n is the refractive index in the *y* direction (n = 1.57). From Eq. (4), we find R = 4.92%. Next, the transmitted part will encounter the second surface and part of the light will be reflected back. The overall transmittance through the two surfaces can be estimated as:

$$T_y \approx (1-R)^2 \approx 1 - 2R = 1 - \frac{2(n-1)^2}{(n+1)^2}. \quad (5)$$

From Eq. (5), we obtain $T_y \approx 90.16\%$, which matches well with the results calculated by the 4 × 4 matrix method. Also from Eq. (5), to improve the transmittance of *y*-polarized light, one solution is to use lower refractive index materials. Of course, the uniaxial material has to be changed accordingly.

To achieve high reflectance, the employed display light is preferably linearly polarized, such as white light emitting diode (WLED)-lit LCD, whose output spectra are shown in Fig. 3(b). From Fig. 3(b), we can see that if we redesign the notched bands at 445nm, 536nm and 610nm and fine-tune the bandwidth, the notched bands can still efficiently cover the output spectra of the display. However, the color gamut of such a WLED-lit LCD is much smaller than that of QD-enhanced LCD. In our design example, we choose QD-enhanced LCDs mainly because of its wide color gamut. This is the new trend for future display systems.

#258893 Received 3 Feb 2016; accepted 29 Feb 2016; published 3 Mar 2016

5. Functional reflective polarizer embedded AR system for color vision deficiency

Our second design example is an AR system with functional reflective polarizer for helping people with color vision deficiency (CVD). For this kind of application, we use the approach shown in Fig. 2(b) with all the three materials discussed in Sec. 3. There are three types of CVD: anomalous trichromacy, dichromacy and monochromacy [10–12]. Our functional reflective polarizer works for people with anomalous trichromacy. For people with normal trichromacy, there are three kinds of cone cells (L, M and S) to perceive colors. Their normalized spectra cone sensitivities are shown in Fig. 4(a) by the solid lines. For people with anomalous trichromacy, one of the three spectra sensitivity functions shifts. Depending on which one of the three spectra sensitivity functions shifts, three types of anomalous trichromacy exist: protanomaly, deuteranomaly, and tritanomaly [25, 26]. For example, in Fig. 4(a), the red dashed lines represent a case of protanomaly where the spectral sensitivity of the L cone cells shifts by 10nm. The larger overlap between the spectra sensitivity functions of the L and M cone cells results in inaccurate color perception. The severity of anomalous trichromacy can be defined as [25]:

$$S = \Delta\lambda / 20, \tag{6}$$

here Δλ is the spectral shift in nm. From Eq. (6), when S = 1, i.e. Δλ = 20nm, which implies that two of the spectra sensitivity functions completely overlap. It means the patient is with dichromacy and can only perceive two primary colors.

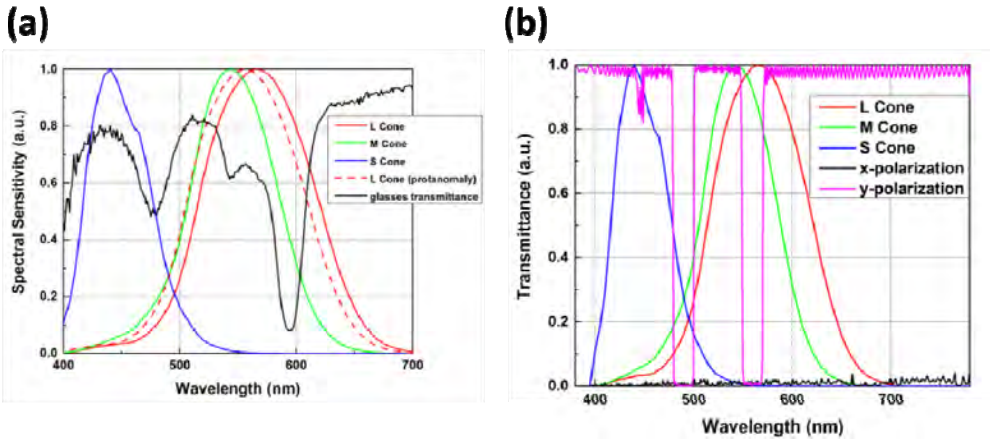

Fig. 4. (a) Spectra sensitivity functions of the L, M and S cone cells and the transmittance of the commercial EnChroma glasses for people with CVD (b) Spectra sensitivity function of the L, M and S cone cells and the transmittance of our functional reflective polarizer in the x and y polarization.

To help people with CVD, both computer algorithm-based approaches [25, 27] and optics-based approaches have been proposed. For the latter, the basic principle is to use notched filters to reduce the overlap between the spectra sensitivity functions of the L, M and S cone cells. Also included in Fig. 4(a), the black line is the measured transmittance data of a commercial EnChroma glass designed for people with CVD. We can see that there are three transmittance dips along the black curve, and these transmittance dips help to reduce the overlap between adjacent spectra sensitivity functions.

In our functional reflective polarizer-embedded AR system, both computer algorithm and optical approaches can be applied to help people with CVD. For the *x*-polarized display light, the display can be tailored based on computer algorithms to adapt to the viewer. The reflectance of the functional reflective polarizer in the *x* direction should be as high as possible, thus it will not temper the output display spectra and cause color inaccuracy of the

#258893 Received 3 Feb 2016; accepted 29 Feb 2016; published 3 Mar 2016

displayed images. For the incident ambient light, the *x*-polarized part will be reflected back and cannot be perceived by the viewer. While for the *y*-polarization, the functional reflective polarizer functions as a notched filter to reduce the overlap between adjacent spectra sensitivity functions. Thus, the functional reflective polarizer can optically adapt the environment light for people with CVD. Based on the approach shown in Fig. 2(b), we have designed the functional reflective polarizer with its transmittance shown in Fig. 4(b). Here we use all three materials listed in Sec. 3 and the reflective polarizer consists of 793 layers with a total thickness of 30.03 μm. Again, the thickness and alignment of each specific layer are not shown here. From Fig. 4(b) it is obvious that our functional reflective polarizer has low transmittance (high reflectivity) for the *x* polarization across the visible range and it works as a notched filter simultaneously in the *y* direction. The overall reflectivity R_D of the *x*-polarized display light calculated from Eq. (3) is ~99.0%. This indicates that with our functional reflective polarizer, both the display light and ambient light can be tailored to help those people with CVD.

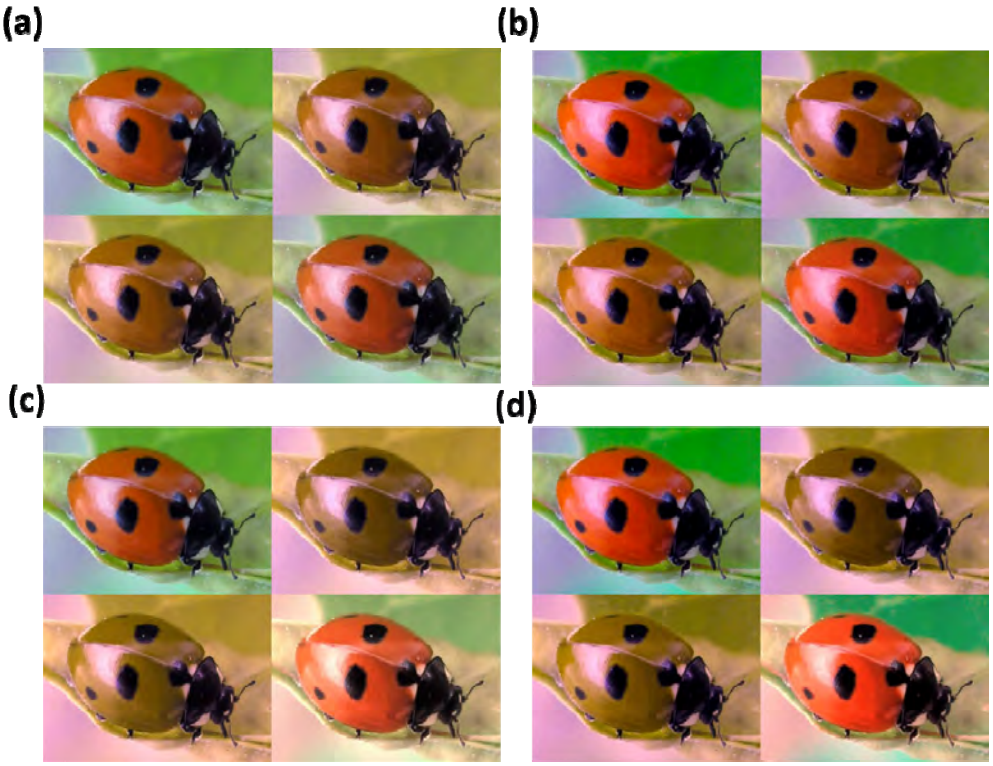

Fig. 5. (a) The perceived image without functional reflective polarizer. From upper left to bottom right, the images correspond to people with normal vision (upper left), protanomaly (upper right), deuteranomaly (bottom left) and tritanomaly (bottom right); (b) the perceived image with functional reflective polarizer. For (a)-(b), the spectral shift is 8nm. (c) The perceived image without functional reflective polarizer when the spectral shift is 16nm and (d) the perceived image with functional reflective polarizer when the spectral shift is 16nm.

To evaluate the performance of our functional reflective polarizer, we simulate the images perceived by people with anomalous trichromacy with and without the functional reflective polarizer. The simulation is powered by the open source isetbio Toolbox [28]. The simulation approach is well documented in [25, 26, 29] and here we summarize it as follows: 1) we obtain the RGB values of each image pixel. By specifying the light source, we can further get the spectra of each image pixel through the isetbio Toolbox. 2) We can simulate the perceived

#258893 Received 3 Feb 2016; accepted 29 Feb 2016; published 3 Mar 2016

spectra of each pixel after the functional reflective polarizer with Fig. 4(b). Then an image perceived by people with normal vision can be reconstructed based on the spectra. For people with anomalous trichromacy, the perceived image can be deduced from the image perceived by people with normal vision based on matrix manipulation described in [25, 26]. Here we assume the ambient environment is a close-up view of a ladybeetle. The simulation image is taken from Wikimedia Commons and here we assume the image is displayed by the OLED panel specified as "OLED-Samsung.mat" in the isetbio Toolbox [28]. In our simulation, we consider two cases: (1) the severity of anomalous trichromacy is 0.4 (8nm spectral shift), which means the anomalous trichromacy is not very severe and (2) the severity of anomalous trichromacy is 0.8 (16nm spectral shift) where the CVD is quite severe. For the first case, the simulation results without and with the functional reflective polarizer are illustrated in Figs. 5(a) and 5(b), respectively. Our functional reflective polarizer helps people with anomalous trichromacy to see more saturated colors when the anomalous trichromacy is not severe. For the second case, the perceived images without and with functional reflective polarizer are demonstrated in Figs. 5(c) and 5(d), respectively. By comparing these two figures, we find that even when the anomalous trichromacy is severe our functional reflective polarizer is still helpful to enhance the image contrast.

The ultimate goal of CVD correction is to enable those people to perceive exactly the same image as a normal person. This, however, cannot been achieved by contemporary computer algorithms or optical approaches. For the optical approaches, the main problem is that even for the same color, the reflection spectra will be different under different lighting conditions. Even so, our functional reflective polarizer can still help people with CVD as it tends to increase the image contrast and color saturation. These two features are important in helping people with CVD. First, higher contrast makes it easier for people with CVD to distinguish between different objects. At the same time, it is easier for people with CVD to distinguish between more saturated colors. Last but not least, because of the Helmholtz-Kohlrausch (H-K) effect [30, 31], people psychologically prefer more saturated colors as they tend to look brighter.

6. Angular performance of the functional reflective polarizer

The working principle of the functional reflective polarizer is based on angular dependent constructive/destructive interferences. Thus, its performance could be degraded at large incident angle. Here we analyze the two functional reflective polarizers mentioned above to see their angular performance. Results are shown in Fig. 6.

For the functional reflective polarizer for inconspicuous AR system and vehicular display, Figs. 6(a)-6(b) depict the angular dependent transmittance for the *x*-polarized light and *y*-polarized light, respectively. From Fig. 6(a) we can definitely see the blue shift on the transmittance curve. However, when the incident angle increases from 0° to 10°, the transmittance curve change is ~2nm and the *x*-polarized display light will still be efficiently reflected by the functional reflective polarizer. From Fig. 6(b), the functional reflective polarizer works like a broadband transmission film for the *y*-polarized ambient light. As the incident angle increases from 0° to 30°, the overall transmittance of the *y*-polarized light is still quite high. Considering that the ambient light is broadband and the *y*-polarized ambient light is dominant in the viewer's perception, we can safely say that this functional reflective polarizer works reasonably well for the incident display light from 0° to 10° and incident ambient light from 0° to 30°.

Similarly, for the functional reflective polarizer used in AR systems for CVD, the angular dependent transmittance is depicted in Figs. 6(c) and 6(d) for the *x*-polarized and *y*-polarized light, respectively. As illustrated in Fig. 6(c), for the *x*-polarized display light, this functional reflective polarizer has low transmittance and high reflectivity from 0° to 30°, which means the functional reflective polarizer can efficiently preserve the specially tailored display image for people with CVD. Meanwhile, for the *x*-polarized ambient light, Fig. 6(c) indicates that it

#258893 Received 3 Feb 2016; accepted 29 Feb 2016; published 3 Mar 2016

can be efficiently reflected back. As for the broadband ambient light in the *y* direction, from Fig. 6(d) we can see that when the incident angle increases from 0° to 30°, the transmittance curve will shift toward blue by ~20nm. Even so the functional reflective polarizer can still effectively reduce the overlap between the spectra sensitivity function of the L, M and S cones, especially between the L and M cones. This suggests the functional reflective polarizer can still help people with CVD at relatively large incident angles.

Overall speaking, our functional reflective polarizers can work at a relatively large incident angle. For both functional reflective polarizers, to improve the angular performance of the whole AR system, we have proposed following approaches:

1. From the display part, we can use a display with relatively broadband output spectra, e.g. WLED-LCD. Thus at large incident angle, the blue-shifted notched band can still cover the output spectra of the display. In this way, the reflectivity for the display light is still high. The main drawback of this approach is that the broadband display leads to a smaller color gamut.

2. The major challenge of our functional reflective polarizer is that the notched bands are usually narrow, and thus the blue shift in transmittance becomes obvious at a large incident angle. Meanwhile, from Figs. 6(b) and 6(c) we can see that when the transmittance/ reflectance curve is broadband at normal incident angle, the problem of blue shift is less severe. For this reason, we can deliberately design some relatively broad notched bands to reduce blue shift.

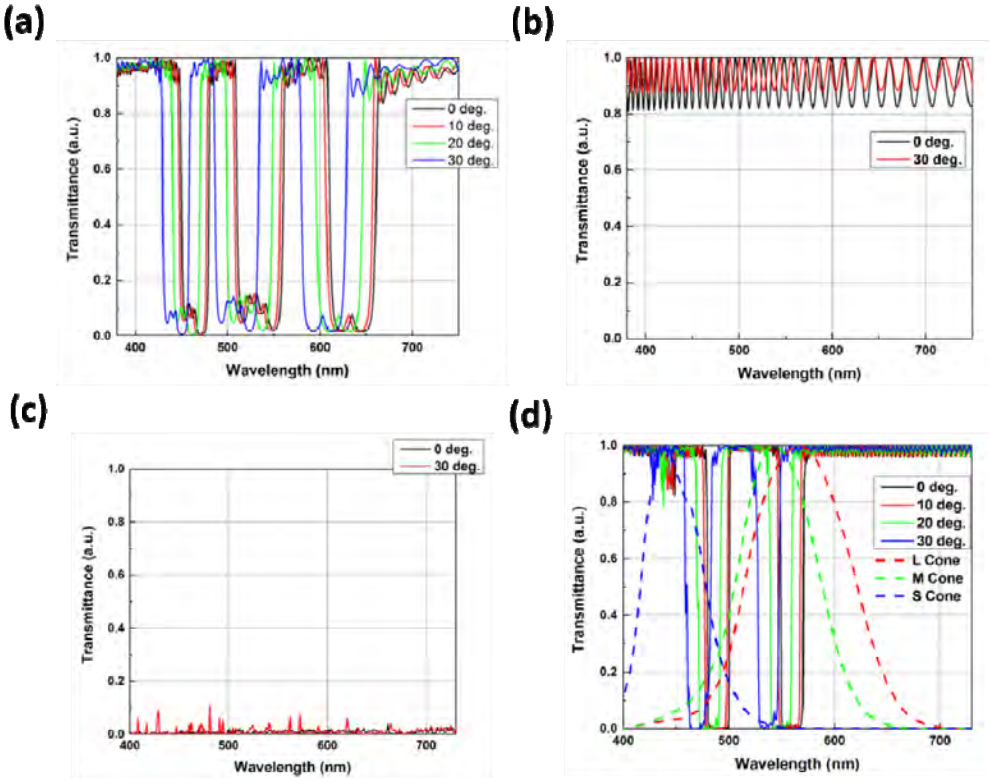

Fig. 6. The angular dependent transmittance of the functional reflective polarizer for inconspicuous AR system in the (a) x direction and (b) y direction; and the angular dependent transmittance of the functional reflective polarizer for people with CVD in the (c) x direction and (d) y direction. Also shown in Fig. 6(d) are the spectra sensitivity function of the L, M and S cone in dashed line.

#258893 Received 3 Feb 2016; accepted 29 Feb 2016; published 3 Mar 2016

In a real AR system, the functional reflective polarizers should be designed according to targeted application, display output spectra, efficiency and angular performance of the display and ambient light. Compromises maybe needed in order to achieve ultimate viewer's experience.

7. Conclusion

We have designed two new functional reflective polarizers based on thin film coating optimization and 4 × 4 matrix method. For the first functional reflective polarizer, it has higher transmittance compared to conventional reflective polarizer, which is ideal for inconspicuous AR system and vehicular display. For the second functional reflective polarizer, it improves the color performance and can be used in an AR system specially designed for people with color vision deficiency.

Acknowledgments

The authors are indebted to Yun-Han Lee and Haiwei Chen for useful discussion about the 4 × 4 method, and AFOSR f or partial financial support under contract No. FA9550-14-1-0279.

#258893 Received 3 Feb 2016; accepted 29 Feb 2016; published 3 Mar 2016